Hydraulic Performances of a Vertical Gate to Effluxes

By

Yoshiaki IWASA* and Hiroshi NAGO*

(Received December 28, 1967)

This paper concerns hydraulic performances of a vertical gate to free and submerged underflows in the light of the one-dimensional treatment of hydraulic analysis. For the free underflow, main emphasis is placed on the contraction of efflux influential to the stage-discharge relationship for practical uses, through a thorough research of past works added to by further experimentations by the authors. A possible scale effect in physical simulation for the present problem will be also explained. For the submerged underflow, the transition problem from free to submerged flow at the gate will be accented. Some discussions of the discharge coefficient of the gate to the submerged underflow are also made.

1. General Scope of Problem

Any type of gate performs substantially as the man-made control structure and gives the flow a hydraulic classification between underflow and overflow in the behaviour. Most practices use the gate as the underflow passage structure, whereas some gates will be operated as the overflow passage structure and in rare cases a combined system of underflow and overflow will be used for the gate structure.

Hydraulic performances of the gate for free underflow passage are commonly made on the empirical basis supplemented by the one-dimensional explanation for the flow pattern. The discharge coefficient of a gate for the underflow and the contraction coefficient of efflux due to a discontinuity in boundary geometry as representative parameters of the classical efflux problem are then made in terms of the geometric ratio of gate opening and upstream depth or specific head. Past experiences give the knowledge that no unified formulation to the efflux problem has succeeded and furthermore predict [1] that a possible scale effect in physical simulation of effluxes would exist. For the submerged underflow characterized by a more complicated flow pattern, similar explanations for the hydraulic performance of the gate will be impossible. Some classical treatments in theoretical

* Department of Civil Engineering

hydrodynamics by means of the irrotational potential theory give mathematical solutions for the contraction coefficient and then for the discharge formula. However, a large variety of experimentations can not verify any mathematical solution in a successful agreement.

Reviewing past knowledge obtained by theoretical and experimental works, it will be noticed that a complete understanding of the efflux problem through physical and mathematical simulations would be impossible. In reality, however, any approach to hydraulic explanation for the performance of gates in efflux problems is anticipated and accelerated by recent technical requests in water resources engineering.

2. Hydraulic Performances of Free Underflow

The main subjects for hydraulic characteristics of the free underflow from a vertical gate are the establishment of discharge formula for underflow and the contraction effect of gate to effluxes.

(1) Discharge Coefficient for Free Underflow In a classical problem on the efflux of flow from a vertical gate, the discharge formula is a solution of simultaneous systems of continuity equation and energy equation in the one-dimensional method of hydraulic analysis and it is commonly

$$q=\frac{\mu a}{\sqrt{\alpha_2+k-\alpha_1\left(\frac{\mu a}{h_1}\right)^2}}\sqrt{2gh_1\left(\lambda_1-\frac{\lambda_2\mu a}{h_1}\right)} \qquad (1)$$

where

q : discharge per unit width
h_1 : upstream uniform depth
a : gate opening
μ : contraction coefficient of free underflow
g : acceleration of gravity
λ_i : pressure distribution coefficient of Jaeger at section i ($i=1, 2$), and subscripts of 1 and 2 indicate up- and downstream sections, respectively
α_i : energy correction coefficient of Coriolis at section i
k : head loss coefficient in terms of downstream velocity

and other symbols are seen in Fig. 1. Nevertheless, Eq. (1) can not be a unified expression for the efflux problem, because of uncertainties of μ, α_1, α_2, λ_1, λ_2, and k in hydraulic behaviours. The discharge formula is commonly given by

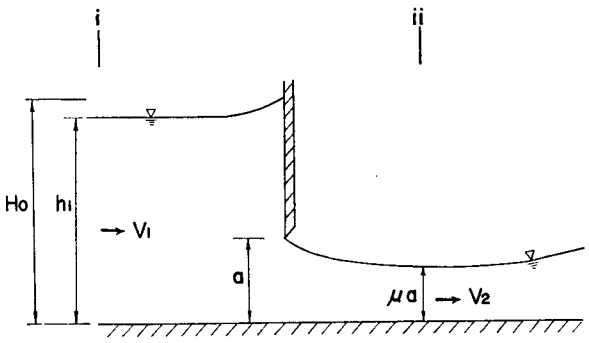

Fig. 1. Free Underflow.

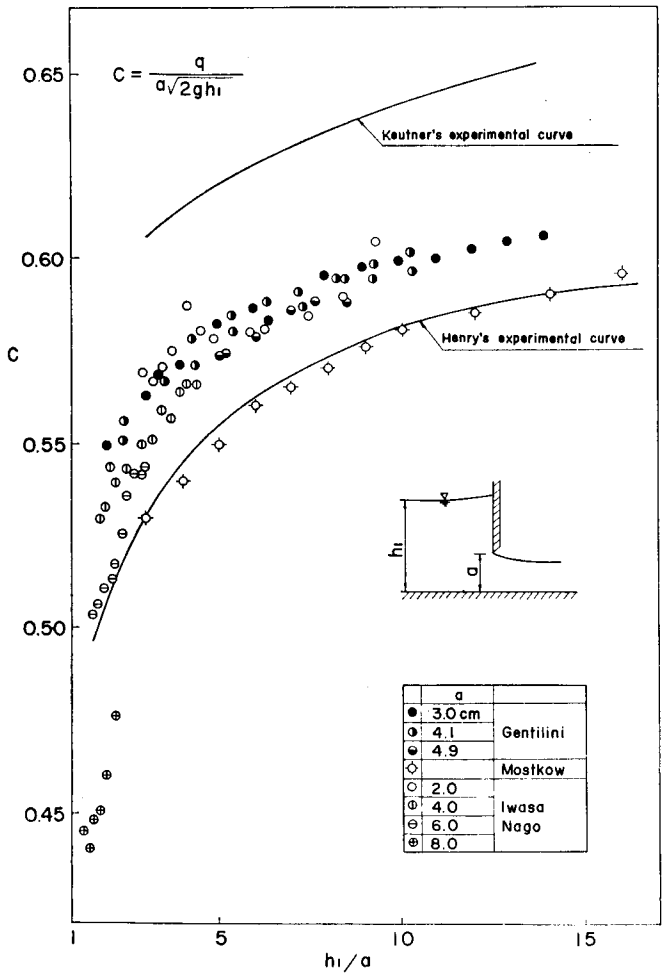

Fig. 2. Discharge Coefficient.

$$q = C \cdot a\sqrt{2gh_1} \tag{2}$$

where C is the discharge coefficient and must be expressed in terms of μ, α_1, α_2, λ_1, λ_2, and k, as seen in Eq. (1).

Past observations of Keutner [2], Mostkow [3], Gentilini [4], Henry [5], supplemented by the experiment of the authors, are plotted in Fig. 2, which predicts an extreme complexity for the expression of discharge coefficient even at a constant value of (h_1/a). Detailed investigations will give following informations:

1. Observing the data obtained by the authors, the discharge coefficient becomes smaller with the increase of gate opening at a constant value of (h_1/a), which predicts that there would be some scale effect of models to the flow behaviour.

2. Comparing the data of Keutner with those of Gentilini and the authors at the same value of gate opening (a=4 cm), an obvious distinction will be seen. The three-dimensional effect of channel geometry to the discharge characteristics will result, because the width of test flume used by Keutner is 1.0 m, whereas that of Gentilini is only 0.16 m and that of the authors 0.20 m.

3. Hydraulic conditions used in the experimentations of Henry and Mostkow have not been known, so that any comparison is not possible.

In a conclusive description after making a glance at the past knowledge in reference to the present problem, the careful use of discharge coefficient to estimate a real value of discharge in prototypes and models is requested in practice.

(2) Evaluation of Contraction Coefficient and Experimental Verification

Concerning the theoretical evaluation of the contraction coefficient of efflux, predominant procedures in mathematical analysis are classical hydrodynamic treatments, in which the problem will be solved by means of the two-dimensional potential theory. Among a number of works in the past, some typical equations are the following:

Mueller [6]:

$$\frac{a}{h_1} = \mu\frac{a}{h_1} + \frac{2}{\pi}\left[1-\mu^2\left(\frac{a}{h_1}\right)^2\right]\tan^{-1}\left(\mu\frac{a}{h_1}\right) \tag{3}$$

Pajer [7]:

$$\frac{1}{\mu} = 1 + \frac{2}{\pi}\frac{1+\lambda^2}{1-\lambda^2}\varepsilon\cot\varepsilon \tag{4}$$

where

$$\varepsilon = \tan^{-1}\frac{2u_1}{u_1^2-1}$$

$$\lambda^2 = \frac{\sqrt{1-(\mu a/h_1)}-\sqrt{1-(a/h_1)}}{\sqrt{1-(\mu a/h_1)}+\sqrt{1-(a/h_1)}}$$

$$\frac{1}{v_1} = \frac{1}{k}\left(u_1 - \frac{\lambda^2}{u_1}\right)$$

$$k = \sqrt{2g(h_1 - a)} \cdot (1+\lambda^2)$$

Knapp [8]:

$$\mu = 1.060\ \mu_{\text{Koch-Karstein}} \tag{5}$$

Koch-Karstein [9]:

$$\mu = \frac{\left(\frac{\pi}{2} - \frac{a}{H_0}\right)\left(2 - \frac{a}{H_0}\right)}{\left(2 - \frac{\mu a}{H_0}\right)\left[\left(\frac{\pi}{2}+1\right) - \left(\frac{\pi}{4}+1\right)\cdot\frac{a}{H_0}\right]} \tag{6}$$

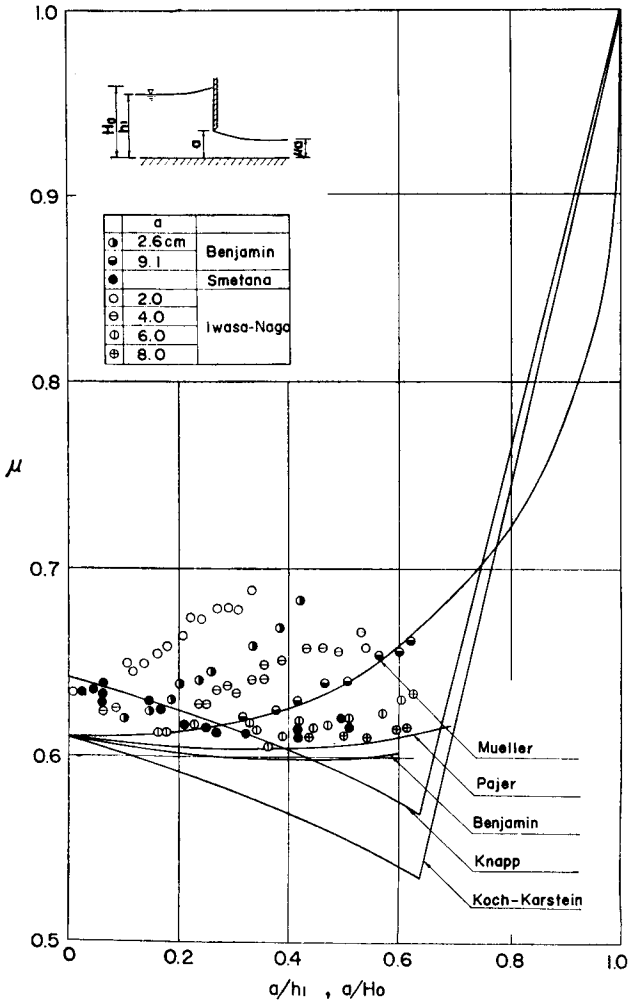

Fig. 3. Contraction Coefficient.

All the equations described in the preceding have been derived by the theoretical treatment for assumed mathematidal models, except that of Knapp. A similar solution obtained through combination of the curve of Pajer and the profile of solitary wave is also proposed by Benjamin [10]. Fig. 3 indicates the behaviours of μ with the increase of (a/h_1) or (a/H_0), expressed by various equations. Experimental data of Smetana [8], Benjamin [10] and the authors are also plotted in the same figure.

Reviewing graphical plottings of theoretical estimation and data observed in Fig. 3, the following conclusions will be found:

1. All observed data are larger in values of contraction coefficient than theoretical predictions except Mueller's, and

2. at a constant value of (a/h_1), actual values of μ obtained through experimentations of Benjamin and the authors decrease with the increase of gate opening and approach the theoretical prediction at large openings.

The first conclusion will be caused by the curvature effect of streamline due to the tip roundness and by the dead water immediately upstream from the gate. The second conclusion will be more informations about the scale effect of model to the flow pattern, which will be treated as the main subject of this section.

The geometric similitude between the model and the prototype has been ascertained in all past experiments, if the flow simulated will be assumed to be two-dimensional. Hence, the prediction of the scale effect requests the uncertainties of kinematic and dynamic or both similitudes. First will concern the velocity distributions in the upstream reach at various gate openings of $a=4.06$, 6.06 and 7.98 cm, as an examination of kinematic similitude. In all cases, the opening ratio to the upstream depth (a/h_1) is constant of 1/3. Fig. 4 is a graphical illustration of velocity distributions measured at a section of $(x/a)=50$, where x is the upstream disance from the gate. This section was selected only for practical convenience in measurement. Even at this section, the depth-wise distribution of downstream velocity is of different form, depending on the gate opening, which demonstrates that the validity of kinematic similitude can not be secured. A distinct demonstration of dynamic similitude for the present problem is further difficult, so that all data observed in the past will be graphically plotted as a function of significant dynamic parameters. Fig. 5 uses the Froude number as the dynamic parameter. At a constant gate opening, say $a=2.0$ cm, the contraction coefficient is much influenced by the Froude number, whereas it will become constant for very high supercritical flows. The same trend will be seen in Fig. 6 where the Reynolds number used as the parameter and in Fig. 7 of the Weber number. In past works, the theoretical treatments ignored the effects of viscous and capillary

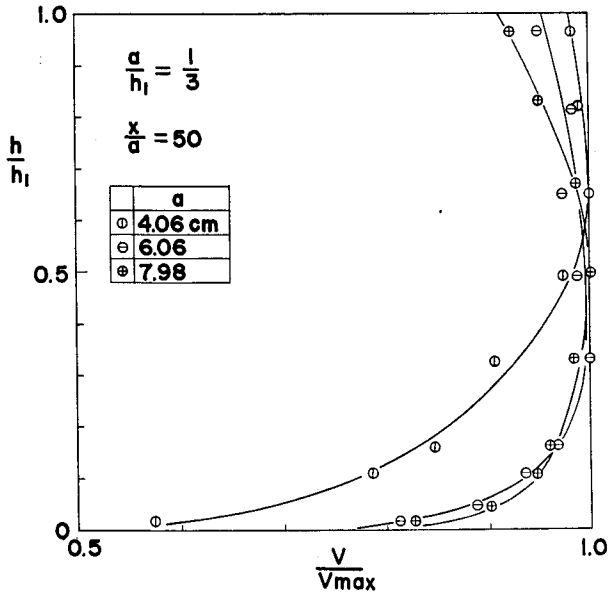

Fig. 4. Velocity Distribution.

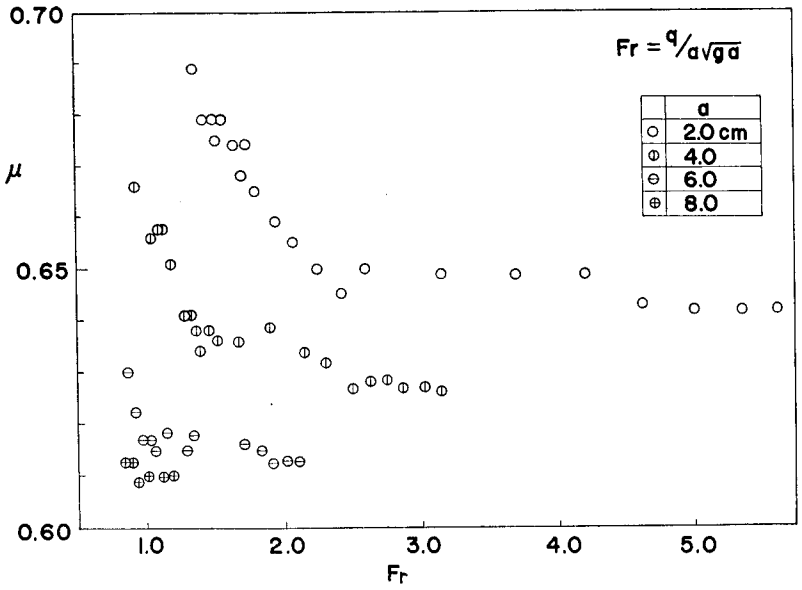

Fig. 5. Contraction Coefficient—Froude Number.

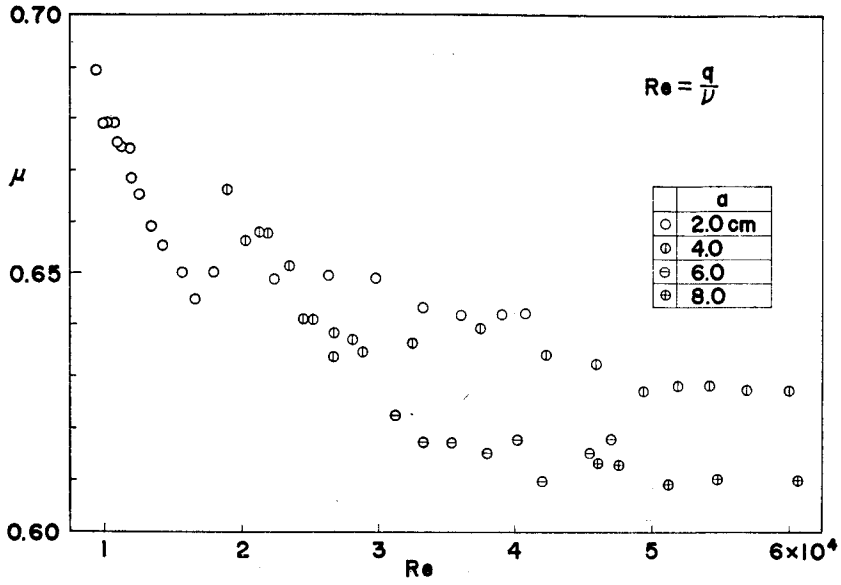

Fig. 6. Contraction Coefficient—Reynolds Number.

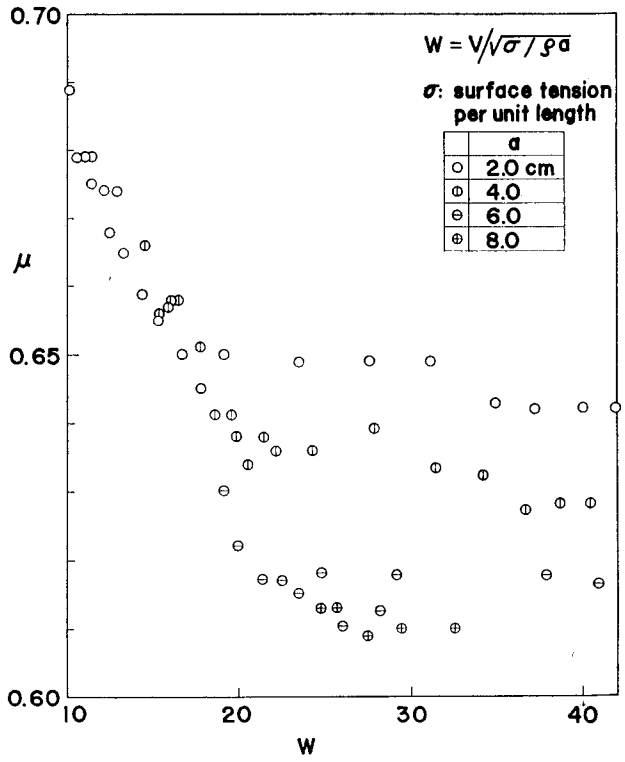

Fig. 7. Contraction Coefficient—Weber Number.

forces, because the basic flow pattern was assumed to be inviscid and irrotational and the capillary force was only set as the boundary condition. Experimental plottings also neglected these effects. A real search for significant parameters and dynamic expressions ascertained by the hydraulic similitude will be still difficult. The only possible way to express the contraction coefficient as a representative of flow pattern will be made by plotting data measured at very large values in Froude, Reynolds and Weber numbers. Fig. 8 is the graphical demonstration of such

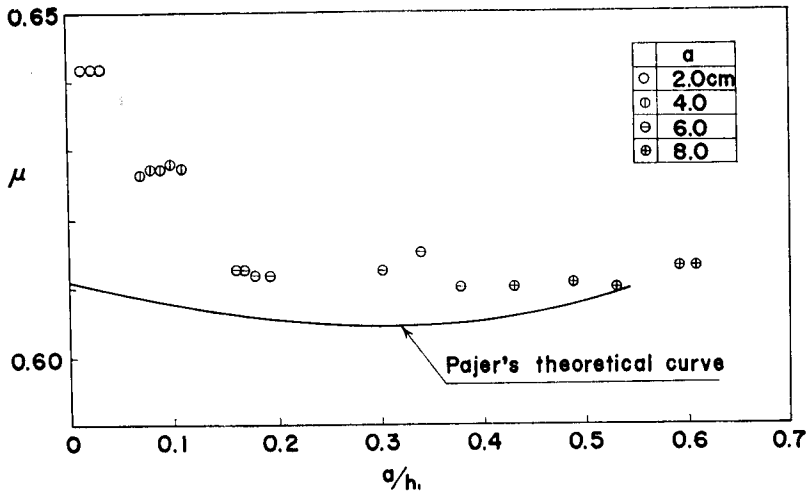

Fig. 8. Contraction Coefficient.

data with the theoretical curve of Pajer. A complete representation for the efflux problem is not still established, as seen in the figure. More detailed experimentations will be requested.

3. Hydraulic Characteristics of Submerged Underflow

(1) One-dimensional Analysis of Hydraulics for Submerged Underflow

The submerged underflow, as schematically illustrated in Fig. 9, is characterized by a more complicated flow pattern combined with efflux and strong eddies. Two distinctly different approaches to analyse the submerged underflow have been made: the classical theory for the one-dimensional flow and the diffusion theory of a jet in a confined flow system. Although each approach has its own preference, the present treatment will be made by the one-dimensional flow theory. A typical model for the submerged pattern of underflow has been proposed by Henry [5] under following assumptions of

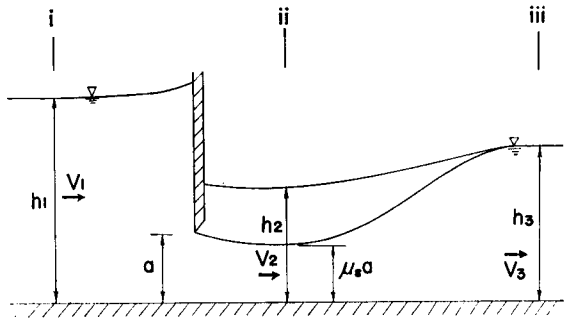

Fig. 9. Submerged Underflow.

1. hydrostatic pressure distributions prevail at all sections in a control volume,
2. between both sections of 1 and 2 in Fig. 9, no energy loss results,
3. at sections of 1 and 3, the uniformity of velocity is secured, and
4. at section 2, the downstream velocity is uniform in the effluxed jet, while that in the horizontal eddy is assumed to be zero.

The simulated model brings the following system of equations:

$$h_1+\frac{v_1^2}{2g}=h_2+\frac{v_2^2}{2g} \tag{7}$$

$$v_2^2\mu_s a+\frac{1}{2}gh_2^2=v_3^2h_3+\frac{1}{2}gh_3^2 \tag{8}$$

$$q=v_1h_1=v_2\mu_s a=v_3h_3 \tag{9}$$

where

h_2: depth of flow at contraction

h_3: downstream uniform depth of flow

μ_s: idealized contraction coefficient for model of Henry

Solutions of the system give the discharge formula, the limit between free and submerged underflow and the like, and the mathematical evaluation and its practical application will be concerned in the next section.

(2) Limit between Free and Submerged Underflow The theoretical limit between free and submerged flow is obtained by inserting $h_2=\mu_s a$ in Eqs. (7) and (8) and it is

$$\left(\frac{h_1}{a}-\mu_s\right)\left(\frac{1}{\mu_s}-\frac{a}{h_3}\right)=\frac{1}{4}\left\{\left(\frac{h_3}{a}\right)^2-\mu_s^2\right\}\left\{\frac{1}{\mu_s^2}-\left(\frac{a}{h_1}\right)^2\right\} \tag{10}$$

The downstream depth of flow h_3 is expressed in terms of the upstream depth of flow h_1, the gate opening a, the Froude number of efflux $q/a\sqrt{ga}$, and the idealized contraction coefficient μ_s.

$$\left(\frac{h_3}{a}\right)^2+2F_r^2\left(\frac{a}{h_3}-\frac{1}{\mu_s}\right)-\left[\frac{h_1}{a}+\frac{F_r^2}{2}\left\{\left(\frac{a}{h_1}\right)^2-\frac{1}{\mu_s^2}\right\}\right]^2=0 \tag{11}$$

The mathematical complexity in estimation of flow behaviours by means of Eqs. (10) and (11) arises from actual values of idealized contraction coefficient. A first approximation will be made by substituting theoretical or experimental values obtained for the free underflow. In this study, the theoretical curve of Mueller is used for predicting the submerged pattern of flow, because the simulated model of Mueller takes a physical preference for the actual submerged underflow comparing with other models. The results are shown in Fig. 10, added by semi-empirical

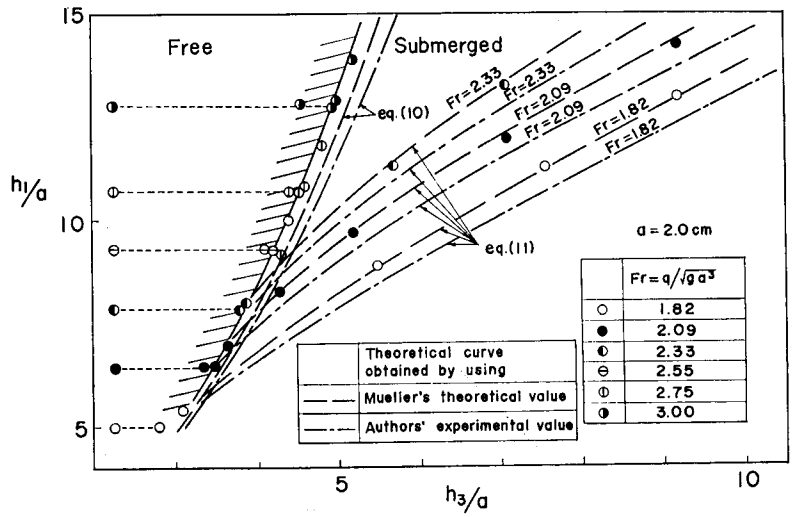

Fig. 10. Relationship between Up- and Downstream Depth of Flow.

curves used observed contraction coefficients. The relationship between up- and downstream depths of flow will be well verified by the theoretical prediction of Mueller. However, the limit between free and submerged flow is not still ascertained. A more exact model for the actual pattern of submerged underflow must be developed.

(2) Discharge Coefficient for Submerged Undderflow The discharge coefficient for the submerged underflow is expressed by

$$C_s=\frac{\mu_s}{\sqrt{1-\left(\frac{\mu_s a}{h_1}\right)^2}}\sqrt{1-\frac{h_2}{h_1}} \tag{12}$$

The experimental verification to Eq. (12) has been made under the following hydraulic conditions of

run	1	2	3	4	5	6	7	8	9	10
h_1 (cm)	10.87	15.70	7.65	12.91	17.58	15.21	19.93	10.17	17.14	18.45
h_2 (cm)	9.68	13.72	5.00	9.22	13.38	8.56	13.27	2.14	7.83	6.69
F_r	1.04	1.85	0.68	1.18	1.61	1.88	2.22	0.93	1.26	1.61

Fig. 11 shows results obtained. During all the test runs, the contraction section was assumed to be at the section of $2a$ in a downstream distance from the gate. The figure shows a good prediction of the Mueller's theory to hydraulic behaviours of submerged underflow for practical uses.

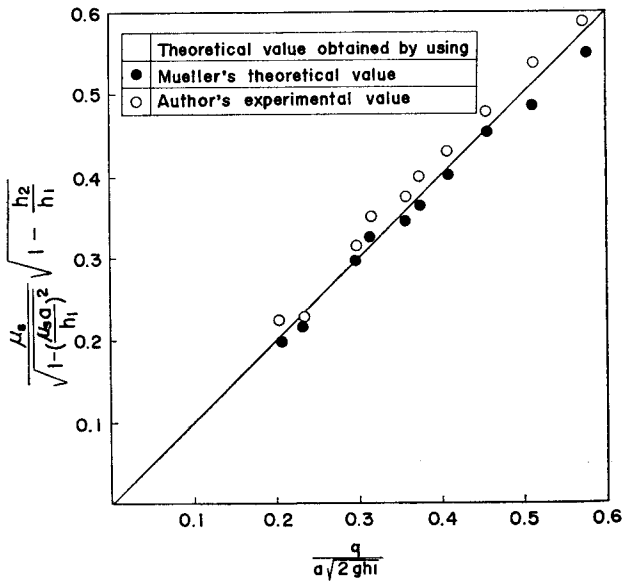

Fig. 11. Discharge Coefficient.

References

1) Iwasa, Y. and H. Nago: Proc. U.S.-Japan Seminar on Similitude in Fluid Mech. (1967)
2) Keutner, C.: Bautechnik, **21**, (1932)
3) Mostkow, M.A.: Handbuch der Hydraulik, VEB, Berlin (1956)
4) Gentilini, B.: Energia elettrica (1941)
5) Henry, H.R.: Proc. ASCE, **75**, (1949)
6) Mueller, H.: Wasserkraft und Wasserwirtschaft (1935)
7) Pajer, G.: ZAMM, **5**, (1937)
8) Knapp, F.H.: Aussfluss, Ueberfall und Durchfluss in Wasserbau, Verlag G. Braun, Karlsruhe (1960)
9) Koch, A. and M. Karstein: Von der Bewegung des Wassers und den dabei auftretenden Kraeften, Verlag J. Springer, Berlin (1926)
10) Benjamin, T.B.: Jour. Fluid Mechanics, **1**, (1956)